RSC Advances

ROYAL SOCIETY OF CHEMISTRY

www.rsc.org/advances

Cite this: DOI: 10.1039/c0xx00000x

www.rsc.org/xxxxxx

ARTICLE TYPE

Synthesis, characterization and environmental application of silica grafted photoactive substances isolated from urban biowaste

Maria Luisa Testa, *[a] Maria Laura Tummino, [a,b] Silvia Agostini, [b] Paola Avetta, [b] Francesca Deganello, [a] Enzo Montoneri, [c] Giuliana Magnacca [b] and Alessandra Bianco Prevot *[b]

Received (in XXX, XXX) Xth XXXXXXXXX 20XX, Accepted Xth XXXXXXXXX 20XX
DOI: 10.1039/b000000x

A waste derived photoactive substance sourced from the green fraction of urban refuses (CVT-230) was immobilized on different types of silica support, one amorphous and other two with controlled porosity (HMS and SBA). In this fashion, three hybrid systems were obtained, which contained CVT as insoluble photoactive principle. They were tested in the photodegradation of 4-methylphenol in aqueous solution irradiated by simulated solar light and promoted the total photodegradation of the pollutant. The materials, both before and after irradiation, were characterized by high-resolution transmission electron microscopy (TEM), small angle X-ray scattering (SAXS), N_2 gas-volumetric adsorption, infrared spectroscopy (FTIR) and thermo-gravimetrical analysis (TGA). The SBA silica hybrid system showed the best performance in terms of stability and reusability, after multiple irradiation cycles. This behaviour can be correlated to the silica morphology and texture capable to better allocate and stabilize the CVT molecules.

Introduction

Over the last few years, a main cause for concern has been the environmental damage provoked by wastes accumulation and by soil, water and air pollution. Proper recycling and reusing of wastes has become mandatory for the sustainable development of our society. In this context, technological development of both urban biowastes (UBW) processing and products for environmental remediation is an important societal challenge. Recently, several papers have reported that the recalcitrant lignin-like fraction of fermented UBW is a cost effective source of soluble bio-based substances (SBO) which can be applied in disparate fields [1, 2]. Depending on the origin and treatment of the sourcing UBW, different SBO can be obtained, showing a wide range of chemical compositions and properties. These substances can be considered as supramolecular assemblies with 76-463 kD weight average molecular weight. They contain long aliphatic chains, aromatic rings and several functional groups as carboxyl, primary and substituted amine and amide, carbonyl, hydroxyl, phenol, ether or ester. SBO have been reported to bear chemical similarities with humic substances, and to exhibit surfactant behaviour [1] and photosensitizing properties [3]. Photosensitizers have been demonstrated to be quite effective in enhancing the photodegradation of water pollutants and promoting significant mineralization of organic carbon.. Interestingly, other workers [2] have shown that the same SBO applied to soil enhances the plant photosynthetic activity. These authors, discussing their results on plant photosynthesis in comparison with those published on the photochemical degradation of organic pollutants in industrial effluent [3], have proposed that SBO might promote either carbon fixation or mineralization, according to the different operational environments. The proposed scenario certainly adds further worthwhile fascinating scope to continue investigating and/or to optimize the performance of SBO as photosensitizers.

Most of the published papers on the photosensitizing properties of SBO deal with a particular type of product (CVT230) which is isolated from urban public park trimming and home gardening residues aged, under aerobic conditions, for 230 days. This product has been tested as homogenous photosensitizer for the degradation of chlorophenols, toxic and not biodegradable compounds found in wastewater, groundwater and soil [3]. The proposed mechanism for SBO photoactivity is based on the mechanisms previously proposed for natural humic substances. It is based on the production, under UV-Vis irradiation, of excited triplet states that can in turn react with the organic substrate by two main mechanisms: hydrogen-transfer and energy-transfer. [4,5] In a previous work [6], concerning the photosensitizing effect of a group of SBO for dyes degradation, hydrogen-transfer was hypothesized as the main mechanism; *i.e*, generated hydrogen atoms can be transferred to the dissolved oxygen with the formation of various reactive oxygenated species, particularly $\bullet$OH and $^1O_2$, which in turn contribute to the degradation of the probe molecule. A further study was devoted to confirm this hypothesis using 4-chlorophenol (4-CP) as probe molecule [7]. The reported results show a complete detoxification of the system, encouraging deeper investigation on the SBO activity. One of the most important drawbacks of CVT230 used as photoactive material is its solubility in water and its consequent difficulty to be separated, after the treatment, from the reaction system. On the contrary, the recovery of an insoluble material is easier, less expensive and more eco-friendly. The present research aimed to turn the soluble photoactive CVT230 into an insoluble form by immobilizing it within a suitable water insoluble support. This approach is expected to yield a stable and recyclable material for performing repeated wastewaters photodegradation cycles. This perspective offers a considerable advantage for the engineering of remediation systems operating in a real environment. To achieve this objective, the similarity between SBO and humic substances was considered. Actually, several synthetic routes have been studied for supporting humic acids (HA) onto silica surface in order to exploit the sorbent properties of the hybrid system [8-11]. Depending on the structure of HA, different functional groups were used for the chemical immobilization. Guzci *et al.* [12] used the phenolic groups of HA as linkers, although the reactions for the activation of silica support were troublesome. Moreover, alcoholic groups of HA were grafted on epoxypropyl silica, while amino groups of HA reacted with chloromethylated support [13].

In the present research, the presence of carboxylic moieties in CVT230 was exploited for the preparation of the heterogeneous hybrid system CVT230/SiO_2 (see Scheme 1).

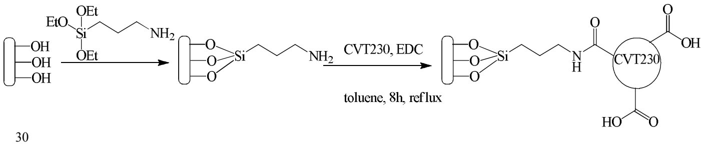

Scheme 1. Synthesis of hybrid organic-inorganic photoactive material

In order to study the role of the silica morphology and textural properties on the photoactivity, CVT230 was grafted on three different types of silica, one amorphous (Am) and the other two with controlled mesoporosity (HMS and SBA-15). The obtained hybrid organic-inorganic materials were, then, characterized by TEM microscopy, small angle X-ray scattering, N_2 gas-volumetric adsorption, IR spectroscopy and thermo gravimetric analysis. The photosensitizing activity, the reusability after one reaction cycle and the stability of the hybrid organic-inorganic materials after several irradiation runs were evaluated using as probe process the degradation of 4-methylphenol (4-MP) in aqueous solution under simulated solar light irradiation.

Experimental

Characterization of CVT230

CVT230 was obtained and characterized as previously reported [2, 14]. It was sourced from a compost of urban wastes and park trimming residues aged for 230 days. This material was hydrolyzed with KOH alkaline water at pH 13 and 60 °C to yield a soluble hydrolysate and insoluble matter. The former was run through an ultra filtration polysulphone membrane with 5 kD cut off. The membrane retentate was dried at 60 °C to yield the final SBO product as black solid in a 15-20 % yield, relative to the starting material. The product had the following C mole % composition: aliphatic C (29.05%); aromatic C (16.03%); anomeric C (6.73%); ketonic C (2.13%); phenolic groups (8.17%); carboxylic acids and amides (11.75%); O-alkyl groups (20.18%); N-alkyl (5.96%). The FTIR spectrum related to the product contained bands at the following wavenumbers: 3360 cm^{-1} (broad, due to OH and NH stretching modes), 2928 cm^{-1} (complex, due to C-H stretching vibration), 1715 cm^{-1} (strong, due to C=O stretching of COOH groups); 1626 cm^{-1} (relative to conjugated C=C groups); 1565 and 1420-1380 cm^{-1} (due to OCO symmetric and asymmetric stretching signals); 1225-1033 cm^{-1} (due to =CH, C-O-C stretching modes). The composition of the CVT230 mineral fraction, after calcination in muffle furnace was determined by ICP analysis and it is expressed as % w/w: Si (2.55±0.01); Fe (0.77±0.04); Al (0.49±0.04); Mg (1.13±0.06); Ca (6.07±0.38); K (3.59±0.21); Na (0.16±0.01).

Sample preparation

For the preparation of the hybrid samples CVT230/SiO_2 a stepwise approach, represented in Scheme 1, was used. First, the silica support was synthesized and the surface was functionalized with aminopropyl groups. Afterwards, the covalent immobilization of CVT230 on aminopropylsilica (AMPS) was carried out using a published method [8] which led to the amide bonds formation by the reaction of AMPS amino groups with the CVT230 carboxylic groups activated by N-(3-Dimethylamino propyl) - N′ - ethylcarbodiimide hydrochloride (EDC).

All the compounds used in the synthesis were purchased from commercial suppliers (Aldrich, Fluka) and used without further purification. Distilled toluene and dimethylformammide (DMF) were stored on molecular sieves (4Å) to assure their complete dryness.

Synthesis of silica support

Different types of silica, hereinafter referred to as Am, HMS and SBA, were synthesized by sol–gel techniques according to published procedures. [15-17]

To obtain the Am, tetraethoxysilane (TEOS, 30 mL, 0.135 mol) was dissolved in ethanol (20 mL) and stirred at 45°C for 15 minutes. Then, 19 mL of aqueous solution of acetic acid at pH 5 was added to the mixture. The temperature was increased to 80 °C until the formation of the gel. The obtained wet gel was dried at 110 °C overnight and then calcined in air at 450 °C/ 4 h.

For the synthesis of HMS, TEOS (12 mL, 0.054 mol) was added to a stirred solution of ethanol (31 mL), water (31 mL) and 1-dodecylamine (3.68 mL, 0.016 mol). The mixture was stirred at room temperature for 24 h. The white precipitate obtained was filtered under vacuum and washed with deionized water (36 mL) and ethanol (36 mL). The solid was dried at room temperature overnight and then calcined in air at 600 °C/ 4 h.

The SBA-15 was prepared by using a non-ionic amphiphilic triblock polymer, Pluronic P123, as surfactant. The polymer (8.1 g) was dissolved in deionized water (146.8 mL) and HCl conc. (37%, 4.4 g) and stirred overnight at 35 °C in a 250 mL one neck flask. TEOS (17.1 mL, 0.077 mol) was quickly added to this solution and stirred for 24 h at 35 °C. The milky suspension was aged at 100 °C for 24 h in a closed polypropylene bottle. The solid product was filtered, washed with a HCl/water mixture and calcined in air at 500 °C/ 5 h (heating ramp of 1 °C/min).

Functionalization of silica with AMPS

Amorphous HMS and SBA silicas were functionalized with aminopropyl groups adopting a grafting method reported in the literature [16]. In a typical procedure, a mixture of 1.00 g of calcined silica in 15.0 mL of dry toluene and 1.00 mL of 3-aminopropyltriethoxysilane (AMPS) was refluxed for 24 h. The material was filtrated *in vacuo*, washed with toluene and dried overnight at 85 °C. The amorphous and the mesoporous grafted silica samples were labelled as NH_2-Am, NH_2-HMS and NH_2-SBA.

Covalent immobilization of CVT230 onto silica

For the immobilization of CVT230 onto silica a procedure used for supporting HA on silica was adopted [11]. CVT230 (435 mg) and EDC (100 mg) were added to a suspension of 1.0 g of amino-functionalized silica in 50 mL of toluene. The mixture was refluxed for 12 h. The material was filtered under vacuum and washed several times with toluene, ethanol and sodium chloride solution (1 M). In order to end-cap the free amino groups and to obtain a stable product, the material was then suspended in 50 mL of DMF containing 5% of acetic anhydride and stirred at room temperature overnight. The product was washed with DMF, H_2O and acetone and finally dried at 85 °C overnight. The immobilized CVT230 materials were labelled as CVT230-Am, CVT230-HMS and CVT230-SBA, respectively.

In order to roughly evaluate the stability of the organic-inorganic hybrid material before its use in photochemical tests, 200 mg of CVT230-Am were suspended in 10 mL of water. The suspension was stirred at room temperature during 8 h and no evidence of CVT230 leaching was found in the clear aqueous solution. The material was then filtered under vacuum and dried at 100 °C overnight. It was recovered as a dry solid in 98.5% yield. The 1.5% loss was likely due to the filtration procedure.

Materials characterization

High-Resolution Transmission Electron Microscopy (TEM) was performed on a JEOL JEM 3010UHR (300 kV) instrument fitted with a single crystal LaB_6 filament. Sample was deposited dry on Cu "holey" carbon grids (200 mesh).

Small angle X-ray Scattering (SAXS) patterns were measured with a Bruker vertical goniometer using Ni-filtered Cu Kα radiation in order to verify the expected ordered porous structure of SBA-15 and CVT230-SBA systems. A proportional counter and 0.05° step sizes in 2θ were used.

The textural properties of samples outgassed at 60 °C for several hours (in order to obtain the standard residual pressure of 10^{-2} mbar in the outgassing system) were obtained using the gas-volumetric apparatus ASAP2020 by Micromeritics. BET method in the standard relative pressure range 0.06–0.2 p/p° allowed to obtain the specific surface areas of the samples before and after the functionalization procedure. The total pore volume, V_p, and the pore size distribution were evaluated by applying DFT model for slit (Am and HMS samples) and cylinder (SBA sample) pores using a low regularization.

FTIR spectra were recorded on a Jasco FTIR 5300 spectrophotometer at the resolution of 4 cm^{-1}, accumulating 100 scans for each spectrum. Self supporting pellet were prepared by 1 mg of sample and 160 mg of KBr, pressing the mixture at 2 ton for 2 min.

Thermo-gravimetrical analyses (TGA) were performed with a TA Instruments TGA 2050 Thermo-Gravimetrical Analyzer in order to assess the amount of organic bonded to the siliceous supports. Analyses were performed on powdery samples under air flow and using a heating ramp of 10 °C/min from 30 to 800 °C. The measurements were performed in aluminium oxide sample holders.

Degradation of 4-Methylphenol

Preliminary experiments were performed on the aqueous solutions of 4-MP at 10 mg L^{-1}, irradiated for 5 and 8 hours in the absence of silica-CVT230, indicated that direct photolysis of the substrate, as evaluated by HPLC measurements of 4-MP. The results showed that the photolysis was not relevant (about 5-7%) compared to the degradation attained in the presence of CVT230-silica hybrid materials. Absorption tests in the dark were also performed by stirring an aqueous suspension of 800 mg L^{-1} of silica-SBO and 4-MP (10 mg L^{-1}) for 4 and 8 hours and then filtering the suspension and analyzing the 4-MP left in solution. The absorbed 4-MP amount can be considered negligible (2-4%). Afterwards, 4-MP photodegradation was studied in the presence of CVT230-silica hybrid materials. Aqueous suspensions of functionalized silica samples CVT230-Am, CVT230-HMS and CVT230-SBA in the concentration range from 80 up to 1200 mg L^{-1} were prepared with ultrapure water (Millipore Milli-Q^{TM} system) and stirred during 30 min before the irradiation. The initial concentration of 4-MP (>99% Aldrich) was kept constant in all the irradiated suspensions and was 10 mg L^{-1}. The photodegradation trials were carried out by irradiating, under continuous stirring, 5 mL of suspensions in a closed Pyrex® cell with a Xenon (1500 W) lamp (Solarbox, CO.FO.Megra-Mi) equipped with a 340 nm cut-off filter. The irradiance of the lamp, measured with a UV-Multimeter system, was 26 W m^{-2}. After irradiation, in order to remove the photoactive material, the samples were centrifuged or filtered through cellulose acetate 0.45 µm pore diameters filter (Millipore).

Degradation of 4-MP was followed by HPLC, employing a Merck-Hitachi instrument, equipped with Lichrospher RP-C18 column (125 mm x 4 mm i.d., d.p. 5µm, from Merck), Rheodyne injector, L-6200 pumps and UV-VIS Merck Hitachi L-4200 detector and D-7000 HPLC System Manager (HSM) software. 4-MP was eluted employing isocratic condition, water (70%) and acetonitrile (30%). The flow rate was 1.0 mL min^{-1}, the retention time was 5.0 minutes and the detector wavelength was 220 nm.

In order to assess the possibility of re-using the CVT230-silica samples the following procedure was adopted: after an irradiation time corresponding to the complete disappearance of 4-MP (15 hours, as reported below in the Results and discussion section), the suspension was centrifuged and the solid was separated and then washed and centrifuged several times. The resulting solid was dried at 50 °C for two days and reused.

A different procedure was chosen in order to age the functionalized silica samples and to evaluate any change in the hybrid materials. A suspension (50 mL) of functionalized silicas (1000 mg L^{-1}) and 4-MP (10 mg L^{-1}) was irradiated in Solarbox for 15 hours. Afterwards, in the same cell, 4-MP (10 mg L^{-1}) was added and again irradiated in the same conditions. This procedure was repeated for a total irradiation time of 45 hours. After each step, the complete abatement of the substrate was verified. At the end of the treatment the samples were recovered, centrifuged, washed with few milliliters of water for two times, dried at 50 °C for two days and characterized. Samples will be indicated as aged (suffix a) in text and figures. For example, CVT230-Am-a indicates the amorphous silica functionalized with CVT230 after 45 hours irradiation in the presence of 4-MP. Organic matter leaching was checked, analyzing the aqueous phase after the separation of functionalized silicas, by UV spectroscopy using a double beam UV-Vis spectrophotometer CARY 100 SCAN-VARIAN with a quartz cell of 1 cm path length.

Results and Discussion

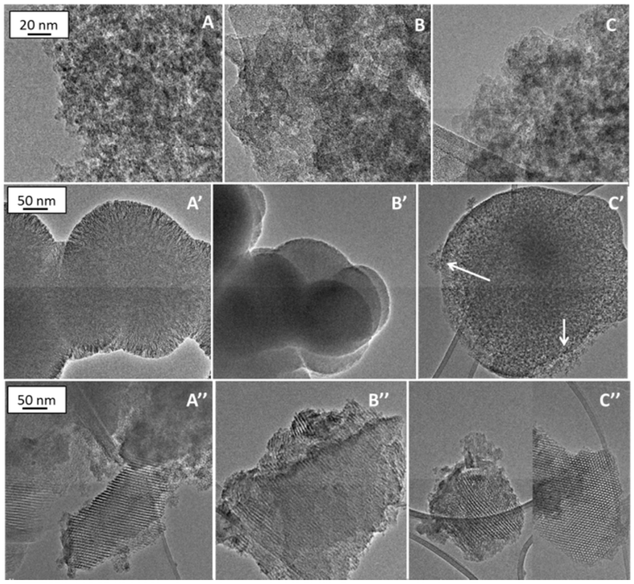

Figure 1. TEM images relative to silicas as prepared (section A), functionalized with CVT230 (sections B) and aged (sections C). From top to bottom: Am, HMS and SBA samples. The arrows in section C' evidence the regions damaged after ageing procedure.

Materials characterization

TEM images are reported in Figure 1 with the best magnification useful to evidence the interesting features of the bare siliceous supports, the fresh and aged hybrid materials. Amorphous silica appear as aggregates of amorphous nanometric particles. After the functionalization with CVT230 some evidences of the presence of the amorphous organic phase can be seen as an undefined halo covering the particles and increasing their aggregation. No significant modification in the morphologic aspect occur after the ageing of the powder.

HMS silica is made of almost spherical particles of 150-400 nm of diameter with a pineapple structure evidencing the radial porosity of the system. After functionalization with CVT230, the pineapple structure is completely lost, probably because the organic phase covers the particles surface and fills the pores. After the photodegradation reactions some structure damages are evident as the material edges are not regular anymore and small amorphous pendants formed around the particles (see arrows in Figure 1 image C').

SBA silica is made of irregularly shaped particles where the regular structure of mesopores appears clearly. The functionalization and the following ageing do not cause any modification in the microscopic appearance of the sample. No changes are visible and the hexagonal structure of the pores is maintained, as evidenced by the image C" of Figure 1.

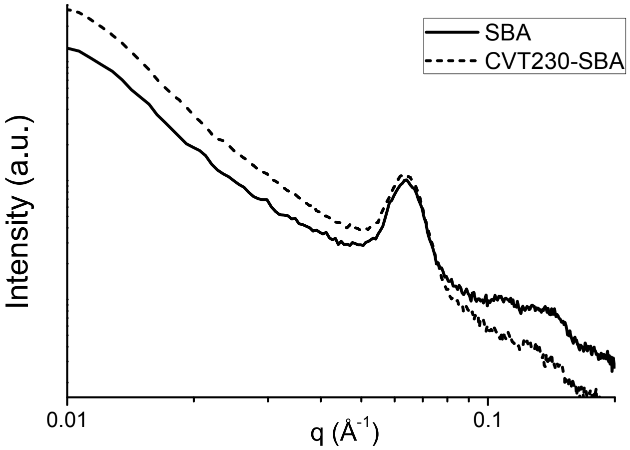

Figure 2. SAXS patterns of SBA and CVT230-SBA samples. X axes are reported in terms of scattering vector, q (using a logarithmic scale). The scattering vector is defined as $|q| = 4\pi\bullet\sin\theta/\lambda$, in which θ is half of the scattering angle and λ is the incoming wavelength.

SAXS patterns of SBA support and CVT230-SBA are compared in Figure 2. SAXS was applied to the bare sample with the aim to evidence the order in pores microstructure and to the functionalized one with the intention to evaluate the effect of CVT230 immobilization on the preservation of the microstructural order. As expected, the SBA diffractogram shows signals at ~0.90 (100), 1.50 (110) and 2.00 (200) °2θ, attributable to hexagonal geometry of cylindrical pores. On the other hand, the CVT230-SBA pattern shows a well-defined signal at 0.90 °2θ, whereas the others two peaks are less intense, indicating a partial loss of the long range microstructural order. Nevertheless, the fact that the signal position remains the same confirms that the porous structure was not modified by the immobilization procedure of CVT230 onto SBA.

Table 1. Textural properties of the prepared materials.

Sample	***BET Surface area (m^2/g)***	***DFT Pore volume (cm^3/g)***	
		< 20 Å	***> 20 Å***
Am	497	0.12	0.38
NH_2-Am	98	0.01	0.20
CVT230-Am	66	< 0.01	0.13
CVT230-Am-a	185	0.01	0.35
HMS	784	0.23	0.15
NH_2-HMS	~ 7	Not measurable	Not measurable
CVT230-HMS	~ 5	Not measurable	Not measurable
CVT230-HMS-a	~ 250	Not measurable	Not measurable
SBA	845	0.40	0.20
NH_2-SBA	147	0.02	0.15
CVT230-SBA	70	< 0.01	0.09
CVT230-SBA-a	~ 300	Not measurable	Not measurable

The data obtained by N_2 gas-volumetric adsorption are collected in Table 1 and Figure 3 for the bare silicas and the corresponding aminopropyl and CVT230-functionalized powders.

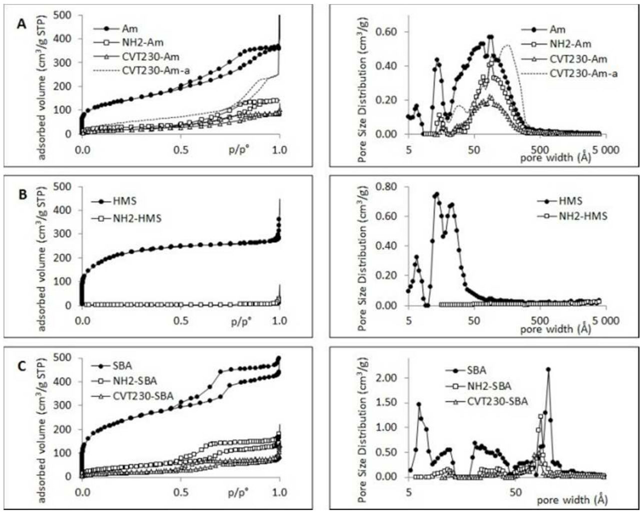

Figure 3. Isotherms (left sides) and pore size distribution curves (right sides) relative to Am (section A), HMS (section B) and SBA (section C) materials as prepared, after aminopropyl grafting and after CVT230 functionalization. The dotted-line isotherm reported in section A is relative to sample CVT230-Am-a.

Unexpectedly, the amorphous (Am) material presented porosity in the micro and meso-range (< 20 Å and > 20 Å of width, respectively). This porosity is not due to the presence of pores inside the particles (the particles are very small if compared with the porosity observed), but is assignable to aggregation of particles and therefore to interparticle void spaces. HMS showed the typical mesoporosity expected for this material, *i.e.* pores of 20-30 Å of diameter [18] and some micropores with diameters less than 20 Å. Ordered mesopores visible at ~100 Å were evidenced in the SBA sample together with a complex distribution of pores (essentially micropores and small mesopores) [19].

As expected, in all cases the grafted samples showed a decrease of surface area and porosity, already visible after aminopropyl functionalization and much more evident after CVT230 immobilization. The effect was dramatic in the case of HMS sample, resulting in the occlusion of all the pores after the aminopropyl functionalization procedure. Otherwise, Am and SBA samples, with different families of pores, showed a selective effect due to the grafting of aminopropyl groups and CVT230 macromolecules. The weight average molecular weight of CVT230 has been estimated 70-80 kD [1]. In the materials containing the grafted CVT230, all the small pores disappeared and the larger ones decreased both in amount and size. In the case of the highly ordered SBA sample, the pore diameters decreased from 100 to 90 Å (after aminopropyl insertion) and to 80 Å (after CVT230 immobilization). These results suggest that the functionalization occludes the small porosity (i.e., pores smaller than 50 Å of width), whereas the larger pores result only partially occupied by grafting molecules.

The morphology of the aged samples was analyzed by N_2 adsorption. The small amount of sample recovered after photodegradation cycles limits the accuracy of the data, but we preferred to avoid mixing samples from different batches to avoid uncertainties due to the treatment and we performed all the analyses on the same starting dose of sample. Nevertheless, in all cases it was possible to observe an increase of the specific surface area. In the case of CVT230-Am-a sample, porosity measurements evidenced an increase of pores' amount and size with respect to the CVT230-Am. These data suggest that a partial loss of the organic phase occurred during the photodegradation reaction.

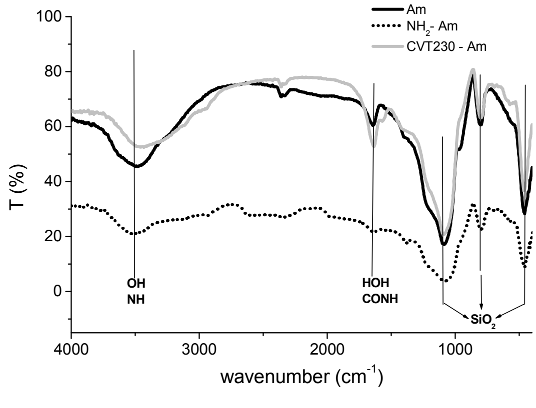

Figure 4. FTIR spectra of the amorphous silica as it (Am, black line), doped with aminopropyl groups (NH_2-Am, dash dot) and after CVT230 grafting (CVT230-Am, gray line)

The FTIR spectra of pure amorphous silica and its derivatives NH_2-Am and CVT230-Am are shown in Figure 4. In all spectra the strong peak at 1100 cm^{-1} is assigned to Si-O-Si asymmetric stretching vibration, while the peaks at 850 and 500 cm^{-1} are characteristic of the Si-OH bending from silica itself. In the silica spectrum, the weak signal at 1630 cm^{-1} is typical of the bending vibration of H-O-H bonds (δ_{HOH}) in physisorbed molecular water, while the broad band at 3500-3600 cm^{-1} arises from the stretching vibration of OH groups interacting via H-bonding. When the aminopropyl groups are grafted on the silica surface, the OH groups signals decrease and NH_2 groups signals appear at ~3400 cm^{-1}. Moreover, the immobilization of CVT230 on silica support was confirmed by the appearance of a strong new peak at 1635 cm^{-1}, typical of the amide group formed by the reaction between NH_2-silica amino groups and CVT230 carboxylic groups. There are not relevant differences among the spectra of the hybrid organic-inorganic samples derived from the different types of silica (Am, HMS and SBA).

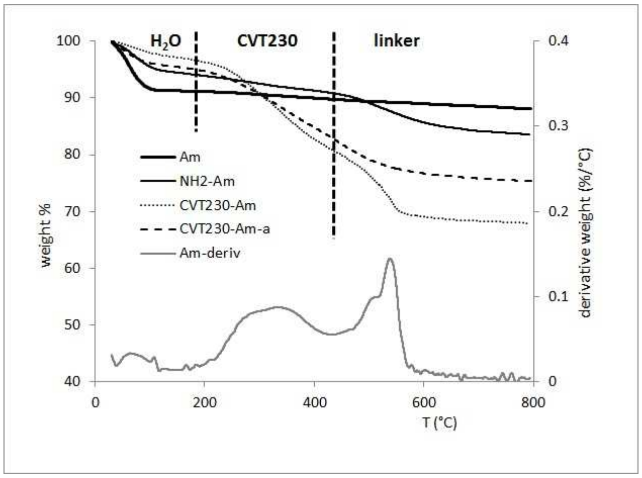

Figure 5. TGA profiles of Am sample as prepared, after aminopropyl (linker) and CVT230 functionalizations and finally after the photoactivated reaction. The grey curve is the derivative of CVT230-Am profile. The dotted lines indicate the temperature range used for determining the release of molecular water, CVT230 and linker groups from the samples.

Table 2. Weight changes (%) of silica samples relative to water (in the range 30-190 °C) and organic release (in the range 190-800 °C). The figures in parentheses indicates the OH release determined as the weight change observed in the range 190-800 °C for the pure silica systems.

Sample	*Water release (%) 30-190°C*	*Organic release (%)*		
		Total amount	*Linker (430-800°C)*	*CVT230 (190-430°C)*
Am	9 (+ 3)	-	-	-
NH_2-Am	6	11	11	-
CVT230-Am	3	29	11	18
CVT230-Am-a	5	20	7	13
HMS	21 (+ 3)	-	-	-
NH_2-HMS	8	15	15	-
CVT230-HMS	8	27	12	15
CVT230-HMS-a	9	29	12	17
SBA	6 (+ 4)	-	-	-
NH_2-SBA	7	13	13	-
CVT230-SBA	7	27	9	18
CVT230-SBA-a	4	26	9	17

All the samples (silicas, aminopropyl-silicas and the CVT230-functionalized materials) were analyzed by means of Thermo Gravimetric Analysis in order to quantify the organic amount bonded during the grafting procedures. As an example, Figure 5 reports the TGA profiles relative to Am sample in the three steps of preparation (bare silica as prepared, aminopropyl silica and CVT230-functionalized sample). Also the profile of the aged material is reported for the sake of comparison. Water and organic amounts evaluated for all the samples are reported in Table 2.

Pure silica presents a main weight loss step in the 30-190 °C range and a second slight weight decrease from 190 up to 800 °C. The first step is certainly due to the loss of physisorbed water, whereas the second weight loss step should be due to the release of water formed from surface OH groups condensation. All the bare silica systems show similar trends except HMS material which presents a relevant amount of water released indicating an important hydrophilic behavior of the system.

NH_2-silica displays two clearly visible steps: the first one in the range 30-190 °C, due to the release of water, and the second one, centered at about 500 °C, due to the thermal degradation of organic matter. In the first step, where a more limited amount of water is released with respect to the bare system, the data in Table 2 are consistent with the lower hydrophilicity of the HMS system as a result of the aminopropyl functionalization. The second step allows to determine the aminopropyl groups (linkers) amount present on the surface of the systems and to evidence a slightly higher functionalization degree for NH_2-HMS system (15% of organic with respect to 13 and 11 % for SBA and Amorphous silica, respectively).

CVT230-functionalized systems (see Figure 5) show a two-steps trend: the first step in the range 30-190 °C is due to water loss. The second step is continuous over the entire 190-800 °C range.

There, it is possible to notice the contribution due to CVT230 loss (190-430 °C) and the aminopropyl elimination (430-800 °C). The amounts relative to the two contributions and the total amount of organic released by materials are reported in Table 2. Lastly, the analysis of aged samples after the photoreaction indicate three different situations: i) the Am sample reflects an important loss of the active phase (ca. 28% of the total amount of CVT230 immobilized on the support is lost); ii) the HMS sample shows an apparent increase of CVT230. There are not logical reasons explaining the organic amount increase after ageing procedure, unless the sample is so modified, as confirmed by TEM images, to make impossible a comparison of the TGA curve before and after prolonged irradiation and contact with 4-MP; iii) the SBA turns out to be the more stable hybrid material with a negligible loss of the active phase after the ageing procedure. This fact could be attributed to the morphology and texture of the SBA support, that allows a better distribution of organic linkers and, as a consequence, of the photoactive CVT230 on the surface support. A similar effect by SBA has been reported in the case of an acid linker containing propyl-sulfonic acid functional groups immobilized onto SBA, HMS and amorphous silica [20]. In that case the SBA hybrid system showed the best performance, due to a better distribution of active sites not only in terms of total amount of linkers but also to the surface density [20]. SBA silica is thus less susceptible to modifications than the other two silica supports, being capable to better allocate organic molecules in its organized porosity, without losing the original microstructural order.

Photodegradation activity

CVT230-Am, CVT230-HMS and CVT230-SBA aqueous suspensions were tested for the photodegradation of 4-MP in water solution. The effect of the CVT230-silica amount, the irradiation time and the CVT230-silica recycling were studied. First of all the 4-MP photodegradation was performed during 6 h runs for all the three CVT230-silica samples varying their concentration in the range 80-1200 mg L^{-1}. This was the result of previous trials indicating 6 hours as a reasonable reaction time.

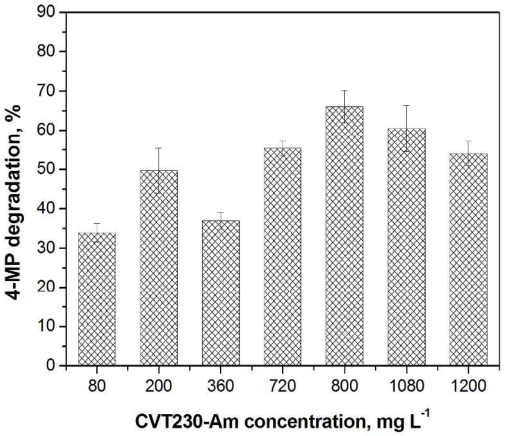

Figure 6. Degradation of 4-MP (10 mg L^{-1}) versus CVT230-Am concentration during 6 h of irradiation.

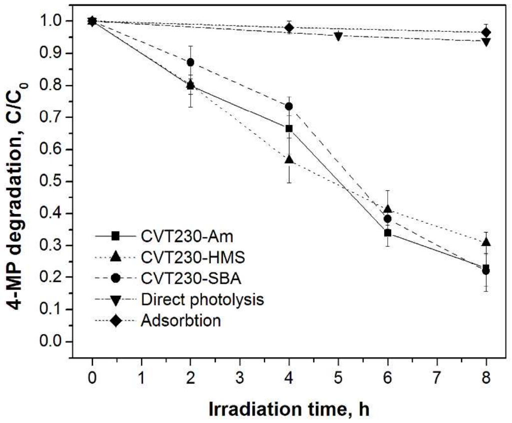

Figure 7. Degradation of 4-MP (10 mg L^{-1}) versus irradiation time in the presence of hybrid organic-inorganic materials (800 mg L^{-1}). Adsoption and photolysis profiles are shown.

Figure 6 reports the percentage of 4-MP degradation versus the CVT230-Am concentration. The degradation efficiency increases with the photoactive material concentration up to about 800 mg L^{-1} and then becomes almost constant in the limit of the experimental uncertainty). Analogous trend were observed also for CVT230-HMS and CVT230-SBA, hence 800 mg L^{-1} was chosen as optimal concentration in order to achieve a good level of degradation without useless excess of hybrid material. Figure 7 shows the kinetic profiles for all the samples during 8 h irradiation time. Moreover, investigations on the adsoption of 4-MP on CVT230-silicas and on 4-MP direct photolysis in pure aqueous solution were carried out. No adsorption and no photolysis was evidenced (see Figure 7). Very similar photodegradation behaviors were observed for the three hybrid materials showing an abatement of about 70-80% of 4-MP after 8 h irradiation. The complete 4-MP disappearance was obtained for all the samples after 15 hours of irradiation. This is consistent with the fact that all samples contained the same amount of grafted CVT230 (Table 2). The results indicate that the photodegradation of 4-MP mainly depends on the photoactive CVT230 immobilized on the silica surface. Hence the degradation could be driven mainly by the photogeneration of reactive oxygenated species rather than by other mechanisms implying substrate adsorption on the CVT230-silica surface. The fact that the activity is directly related to the CVT230 phase, and not to other adsorption phenomena involving the support, can be confirmed observing the effects of a surface area normalization on the degradation activity shown by the three materials. All systems show similar catalytic activity for mass of catalyst, but CVT230-Am and CVT230-SBA possess specific surface areas of about 70 m^2/g, whereas CVT230-HMS shows a specific surface area which is at least 10 times lower than the others. If a normalization is carried out for area of catalyst, one square meter of HMS-based system shows a reactivity which is at least ten times higher than the others. This is possibleonly considering that Am-based and SBA-based systems expose to the substrate not only the active CVT230 phase but also the inactive siliceous support whereas HMS-based system expose to the reaction much more active phase, i.e. an amount at least ten times higher.

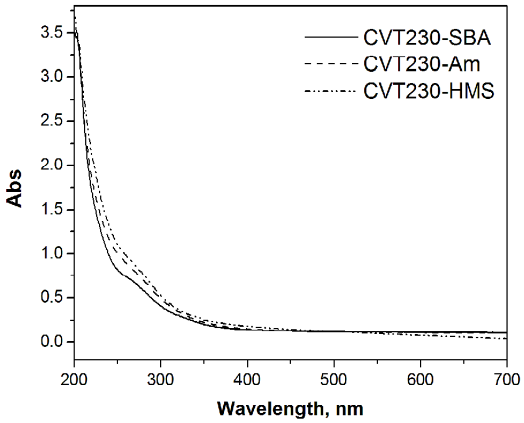

Figure 8. UV-Vis spectra of the aqueous solutions obtained after the separation of the three photoactive materials irradiated in the presence of 4-MP for three cycles (total irradiation time = 45 h).

The possibility of re-using the material after its recovery and resuspension was tested on CVT230-Am: after 6 hours of irradiation the results evidenced that the photoactivity was maintained. To assess the effect of the photoactive material ageing by longer irradiation, three cycles of 15 hours irradiation in the presence of an initial concentration of 10 mg L^{-1} of 4-MP for each cycle were carried out. The complete abatement of 4-MP was always verified. At the end of the third run the material was separated and the UV-Vis spectrum of the solution was recorded (see Figure 8). It may be observed that the absorbance is not negligible. These fact may be caused by partial detachment of material containing CVT230 from the silica support.

Conclusions

For the first time a photoactive bio-based substance (CVT230) was grafted on different silica supports and tested as heterogeneous photosensitizer for the abatement of 4-methylphenol. All materials were able to completely promote the photodegradation of 4-methylphenol. Despite a slight depletion of the organic component, the photoactive performance of the CVT230-silica was not reduced after 15 hours of irradiation, as confirmed upon re-using the material for a second 4-MP degradation trial. The results evidence the best performance and stability for the SBA hybrid material. This is most likely due to the particular morphology and texture of SBA, which best hosts and protects the CVT230 from self-degradation and leaching.

Acknowledgments

The authors are thankful to 7thFP IRSES-2010-269128-EnvironBos Marie Curie Action for funding. Studio Chiono ed Associati in Rivarolo Canavese (TO) and Acea Pinerolese Spa in Pinerolo (TO) are also greatly acknowledged, for supplying the CVT230 and its sourcing material respectively. The scientific activities described in this paper belong to project MAT4TREAT: it has received funding from the European Union's Horizon 2020 research and innovation program under the Marie Skłodowska-Curie grant agreement N° 645551. The authors thank Dr. Francesco Giordano for the SAXS measurements.

Notes and references

[a] *CNR-ISMN, via U. La Malfa 153, I-90146, Palermo, Italy. Fax: +390916809399; Tel +390916809253; E-mail: marialuisa.testa@cnr.it, marialuisa.testa@ismn.cnr.it*
[b] *Università di Torino, Dipartimento di chimica e NIS Centre of Excellence, via P. Giuria 7, I-10125 Torino, Italia. Fax: +39 011 6705242; Tel: +39 011 6707631;E-mail: alessandra.biancoprevot@unito.it*
[c] *Biowaste Processing, Via XXIV Maggio 25, 37126 Verona*

1 E. Montoneri, D. Mainero, V. Boffa, D. G. Perrone and C. Montoneri, *Int. J. Global Environ*., 2011, **11**, 170-196.
2 O. Sortino, E. Montoneri, C. Patanè, R. Rosato, S. Tabasso, M. Ginepro, *Sci. Total Environ.*, 2014, **487C**, 443-451.
3 (a) P. Avetta, F. Bella, A. Bianco Prevot, E. Laurenti, E. Montoneri, A. Arques and L. Carlos, *ACS Sust. Chem. Eng.,* 2013, **1**, 1545-1550; (b) J. Gomis, A. Bianco Prevot, E. Montoneri, M.C. Gonzalez, A. M. Amat, D.O. Martire, A. Arques , L. Carlos. *Chem Eng J*, 2014, **235**,236-243
4 A. Amine-Khodja, O. Trubetskaya, O. Trubetskoj, L. Cavani, C. Ciavatta, G. Guyot, C. Richard, *Chemosphere,* 2006, **62**, 1021-1027.
5 C. Richard, D. Vialaton, J-P. Aguer, F. Andreux, *J. Photochem. Photobio. A*, 1997, **111,** 265-271.
6 A. Bianco Prevot, D. Fabbri, E. Pramauro, C. Baiocchi, C. Medana, E. Montoneri, V. Boffa, *J. Photochem. Photobio. A*. 2010, **209,** 224-231.
7 A. Bianco Prevot, P. Avetta, D. Fabbri, E. Laurenti, T. Marchis, D. G. Perrone, E. Montoneri, V. Boffa, , *ChemSusChem*, 2011, **4**, 85-90.
8 L.K. Koopal, Y. Yang, A. J. Minnaard, P. L. M. Theunissen and W. H. Van Riemsdijk, *Colloid Surface A*, 1998, **141**, 385–395.
9 M. Klavins and L. Eglite, *Colloid Surface A,* 2002, **203**, 47–54.
10 D. Luo, Q.W. Yu, H.R. Yin and Y.Q. Feng, *Anal. Chim. Acta*, 2007, **588**, 261–267.
11 P. Stathi and Y. Deligiannakis, *J. Colloid. Interf. Sci.,* 2010, **351**, 239–247.
12 J. Guzci, A. Angelova, R.A. Bulman and G. Szabo, *React. Polym*., 1992, **17**, 61-68.
13 M. Klavins, L. Eglite and A. Zicmanis, *Chemosphere*, 2006, **62**, 1500–1506.
14 F. Deganello, M. L. Tummino, C. Calabrese, M. L. Testa, P. Avetta, D. Fabbri, A. Bianco Prevot, E. Montoneri and G. Magnacca, *New J. Chem*., 2015, **39**, 877-885.
15 G. Pecchi, P. Reyes, I. Concha and J.L.G. Fierro, *J. Catal*., 1998, **179**, 309–314.
16 A. R. Silva, K.Wilson, J.H. Clark and C. Freire, *Micropor. Mesopor. Mat.*, 2006, **91**, 128–138.
17 M. Choi, W. Heo, F. Kleitz and R. Ryoo, *Chem. Commun.,* 2003, 1340–1341.
18 T. R. Pauly and T. J. Pinnavaia, *Chem. Mater*., 2001, **13**, 987-993.
19 D.Y. Zhao, J. L. Feng Q. S. Huo, N. Melosh, G. H. Fredrickson, B. F. Chmelka and G. D. Stucky, *Science*, 1998, **279**, 548–552.
20 M. L. Testa, V. La Parola, L.F. Liotta, A.M. Venezia, *J. Mol. Cat. A*, 2013, **367**, 69-76.